DOI: https://doi.org/10.15407/pmach2026.03.043

UDC 674.047-043.84:536.423

DRYING KINETICS OF SAL WOOD (SHOREA ROBUSTA): MOISTURE DIFFUSIVITY, ACTIVATION ENERGY, AND BIOMASS ENERGY IMPLICATIONS

[1] Munna Verma
ORCID: 0000-0003-2146-3234

[2] Ravi Kant Ranjan
ravi.me11@nitp.ac.in
ORCID: 0000-0002-4023-689X

[1] Bhagwant University
Ajmer-305004, Rajasthan, India

[2] Government Polytechnic Sahjanwa
Gorakhpur – 273209, Uttar Pradesh, India

This paper investigates the isothermal drying kinetics and effective moisture diffusivity of cylindrical Shorea robusta (Sal) wood particles dried in a hot air oven at 75 °C, 90 °C, and 105 °C. Sal wood, one of the most ecologically and commercially significant hardwood species of the Indian subcontinent, holds considerable promise as a biomass fuel feedstock, yet its drying characteristics have not been systematically characterized. Five established thin-layer drying models; Lewis, Page, Modified Page, Wang & Singh, and Henderson & Pabis, were fitted to the experimental moisture ratio (MR) data using MATLAB curve fitting. The Page model provided the best statistical fit, yielding coefficients of determination (R^2) of 0.9971, 0.9988, and 0.9983; sum of squares of error (SSE) values of 0.003618, 0.001854, and 0.003047; and root mean square error (RMSE) values of 0.01608, 0.01151, and 0.01425 at 75°C, 90°C, and 105°C, respectively. Effective moisture diffusivity, calculated via the analytical solution of Fick's second law for cylindrical geometry, increased from 7.92×10^{-8} to 26.0×10^{-8} m²/s over the experimental temperature range. Activation energy, estimated using an Arrhenius-type equation, was found to be 4.42×10^{4} J/mol, consistent with values reported for analogous lignocellulosic biomasses. The findings provide fundamental kinetic data for rational dryer design and optimisation of biomass pre-treatment systems.

Keywords: *activation energy, drying kinetics, effective moisture diffusivity, hot air oven, thin-layer drying.*

Introduction

The transition from fossil fuels to renewable energy is among the most pressing challenges of the twenty-first century. Lignocellulosic biomass has emerged as one of the most versatile and globally abundant renewable energy carriers, capable of direct combustion, gasification, and pyrolysis, as well as conversion to liquid biofuels [1, 2]. In the Indian subcontinent, woody biomass occupies a central position in rural energy supply chains, supplying cooking fuel, process heat, and increasingly, electricity through decentralised gasification and combustion systems [3, 4]. However, the thermochemical utilisation of woody biomass is significantly impaired by its inherent moisture content, which reduces energy density, increases transportation costs, generates incomplete combustion, and elevates greenhouse gas emissions during end-use [5, 6]. Therefore, pre-treatment drying is an essential and energy-intensive step in virtually all woody biomass supply chains, and an accurate characterisation of drying kinetics is indispensable for rational dryer design and process optimisation [7, 8].

Shorea robusta Gaertn. (Sal), a member of the family Dipterocarpaceae, is the dominant timber and biomass species across the Indian subcontinent, with a natural range spanning the southern foothills of the Himalayas and distributed across Nepal, India, and Bangladesh, covering over 11 million hectares [9]. In India alone, Sal forests extend in a near-continuous belt from Assam and West Bengal through Odisha and Jharkhand to the Shivalik Hills in Haryana, as well as in the Eastern Ghats, Eastern Vindhya, and parts of the Satpura range [10, 11]. Sal is valued not only for its dense, hard timber used in construction, railway sleepers, and furniture, but also as a major source of fuelwood and biomass for rural and peri-urban communities [12]. Pradhan et al. [13] have confirmed Sal seed biomass as a high-calorific, low-ash feedstock with significant pyrolysis potential, while Behera and Misra [14] demonstrated that recovering Sal forests in Eastern India can accumulate above-ground biomass up to 231.9 Mg/ha. The scale and accessibility of Sal Forest biomass render it an important feedstock for decentralised bioenergy applications throughout the region.

Moisture content critically governs the quality and conversion efficiency of woody biomass. For combustion applications, the moisture content must be reduced to 10–15 wt% (wet basis), while gasification sys-

This paper is licensed under a Creative Commons Attribution 4.0 International License.
© Munna Verma, Ravi Kant Ranjan, 2026

tems can tolerate a broader range of 10–65 wt% depending on the gasifier type [15]. Drying roughly doubles the energy density of biomass, from approximately 8 to 20 MJ/kg, by removing bound and free moisture [16]. Without adequate drying, a substantial fraction of the lower heating value is consumed by the latent heat of vaporisation of moisture, reducing combustion efficiency and increasing incomplete-combustion pollutants [17, 18]. Dried biomass also incurs significantly lower packaging, transport, and storage costs, and its physical handling is improved [5]. Castagna and Rein [19] recently demonstrated that moisture content strongly influences not only the calorific performance but also the pyrolysis and burning behaviour of wood, further underlining the importance of controlled drying as a pre-treatment step. From an engineering standpoint, the drying kinetics of a given biomass are fundamental inputs for the rational design of dryers, the selection of operating conditions, and the accurate simulation of biomass supply chains [20].

Thin-layer drying models, which express the dimensionless moisture ratio (*MR*) as a function of time and drying temperature through empirical or semi-theoretical equations, are widely used to characterise the drying kinetics of biomass and agricultural products [21]. These models are computationally inexpensive and readily fitted to experimental data using standard nonlinear regression, making them practical tools for dryer engineering [22]. Gandía-Ventura et al. [23] conducted an extensive review of kinetic models for wood biomass drying in hot airflow systems, concluding that empirical models particularly the Page model consistently provide good fits for woody biomass across a wide range of species and experimental conditions, though they caution that model parameters are species- and condition-specific and should not be extrapolated without experimental validation. This observation reinforces the need for systematic drying kinetics studies on each biomass species of practical relevance.

Researchers have employed hot air oven dryers extensively as controlled laboratory platforms for acquiring isothermal drying kinetic data, free from the confounding effects of variable air velocity and humidity encountered in industrial dryers. Mihindukulasuriya and Jayasuriya [23] characterised the drying behaviour of chillies in a hot air oven and fluidised bed dryer. Safeena and Patil [24] investigated the quality of Dutch rose flowers dried in a hot air oven. Upadhyaya et al. [25] developed empirical drying models for spinach leaves in a hot air oven. Faisal et al. [26] evaluated potato drying in a hot air oven. For woody biomass, Chen et al. [27] determined effective moisture diffusivity and drying kinetics for poplar sawdust under isothermal thermogravimetric analysis conditions, and Sridhar and Madhu [28] modelled the drying kinetics of *Casuarina equisetifolia* wood chips at multiple temperatures. Kuznetsov et al. [29] examined heat and mass transfer during drying of large-thickness wood biomass layers under convective conditions, identifying internal diffusion as the dominant resistance even for macroscopic samples. More recently, Núñez-Retana et al. [30] developed predictive convective drying kinetics models for *Pinus* spp. wood chips, emphasising the role of particle size and temperature on effective diffusivity. Despite this body of work, no study in the published literature has characterised the drying kinetics, effective moisture diffusivity, or activation energy of *Shorea robusta* wood, a species of pre-eminent importance in the Indian subcontinent, at the single-particle level under controlled isothermal conditions.

The present study addresses this gap by pursuing the following specific objectives:

– to experimentally characterise the drying curve of a single cylindrical Sal wood particle in a hot air oven at three temperatures (75 °C, 90 °C, and 105 °C);

– to fit the experimental *MR* data to five established thin-layer drying models and identify the best-fit model through statistical analysis;

– to estimate effective moisture diffusivity using Fick's second law of diffusion for cylindrical geometry;

– to determine the activation energy of the drying process using an Arrhenius-type equation. The outcomes are intended to provide foundational kinetic data for the design of biomass drying systems specifically applicable to Sal wood in the Indian subcontinent context.

1 Material and methods

1.1 Experimental setup and equipment

The experimental configuration of the hot air oven dryer is presented in Fig. 1. The apparatus is an electrically powered, forced-convection unit (capacity: 50 litres). An internal recirculating fan ensures uniform heat distribution throughout the drying chamber. A precision thermostat maintains the set-point temperature throughout each experimental run. The oven incorporates a nichrome heating element, a double-wall insulated enclosure, and a thermocouple positioned at the geometric centre of the chamber. During drying experiments,

the sample was suspended at the centre of the oven using a fine nichrome wire attached to a precision balance (Citizen Scale, Model CY 204; accuracy: ±0.1 mg) mounted externally, enabling continuous gravimetric monitoring without interrupting the drying process.

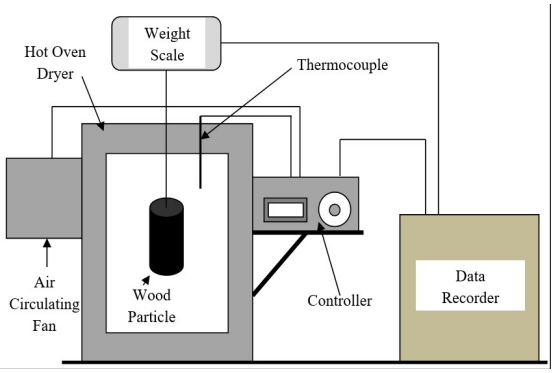


Fig. 1. Experimental set-up of the hot air oven dryer

1.2 Sample preparation and drying procedure

Cylindrical Sal wood samples with a diameter of 20 mm and height of 25 mm were machined from freshly harvested *Shorea robusta* timber. Prior to each drying experiment, the samples were oven-dried at 105 °C for 24 hours to determine the bone-dry mass (W^d). Samples were subsequently immersed in distilled water for 72 hours to achieve full saturation, and the saturated mass was recorded. Drying experiments were conducted at three isothermal temperatures 75 °C, 90 °C, and 105 °C with the oven brought to steady-state temperature before each run. The sample weight was recorded at regular intervals over a 360-minute drying period. Each experiment was replicated three times, and the averaged data were used in all subsequent analyses, consistent with the methodology recommended by Loha et al. [31] for forced convection drying experiments.

1.3 Mathematical modelling of drying kinetics

Moisture content on a dry basis (*MC*), drying rate, and moisture ratio (*MR*) was calculated at each measurement interval. The governing expressions are [5, 27]

$$MC(\%) = \frac{W^b - W^d}{W^d} \times 100\,; \tag{1}$$

$$MR = \frac{M_t - M_e}{M_0 - M_e}\,, \tag{2}$$

where W^b is the wet mass; W^d is the dry mass; M_0 is the initial moisture content (dry basis); M_e is the equilibrium moisture content; and M_t is the moisture content at time t. Since both M_0 and M_t greatly exceed M_e throughout the experiments, Eq. (2) simplifies to [27, 31]

$$MR = \frac{M_t}{M_0}\,. \tag{3}$$

Five widely used thin-layer drying models (Table 1) were fitted to the experimental *MR* versus time data [28, 32–34]. The best-fit model was selected based on three statistical criteria: the coefficient of determination (R^2), sum of squares of error (*SSE*), and root mean square error (*RMSE*), defined as [28, 31]

$$SSE = \left[\frac{\sum_{i=1}^{n} \left(MR_i^{cal} - MR_i^{exp} \right)^2}{N} \right]^{\frac{1}{2}}; \tag{4}$$

$$RMSE = \left[\frac{1}{N} \cdot \sum_{i=1}^{N} \left(MR_i^{exp} - MR_i^{cal} \right)^2 \right]^{\frac{1}{2}}; \tag{5}$$

$$R^2 = 1 - \frac{\sum_{i=1}^{N} \left(MR_i^{exp} - MR_i^{cal} \right)^2}{\sum_{i=1}^{N} \left(\overline{MR}_i^{exp} - MR_i^{cal} \right)^2}\,, \tag{6}$$

where N is the total number of observations; and MR_i^{cal} and MR_i^{exp} are the calculated and experimental moisture ratios at the i^{th} data point, respectively. Model constants were determined using the MATLAB Curve Fitting Toolbox (MathWorks, R2022a). A higher R^2 combined with lower *SSE* and *RMSE* indicates a superior model fit [20, 28].

Table 1. Thin-layer drying models applied in this study

No.	Model Name	Model Equation	Reference
1	Lewis	$MR = e^{-kt}$	Lewis (1921)
2	Page	$MR = e^{-kt^n}$	Page (1949)
3	Modified Page	$MR = e^{-kt^n}$	Wang & Singh (1978)
4	Wang & Singh	$MR = 1 + kt + k_1 t^2$	Wang & Singh (1978)
5	Henderson & Pabis	$MR = a \cdot e^{-kt}$	Henderson & Pabis (1969)

1.4 Effective moisture diffusivity and activation energy

Effective moisture diffusivity ($D^{e\varphi\varphi}$) was estimated using the first-term approximation of the analytical solution of Fick's second law for a cylinder, which is appropriate when the drying occurs exclusively in the falling-rate period [35]

$$MR = \frac{6}{\pi^2} \cdot e^{-\frac{\pi^2 D^{e\varphi\varphi} t}{4h^2}}, \tag{7}$$

where h (m) is the half-thickness of the sample; and t (s) is the drying time. Linearising Eq. (7) by taking the natural logarithm of both sides yields

$$\ln MR = \ln \frac{6}{\pi^2} - \frac{\pi^2 D^{e\varphi\varphi} t}{4h^2} t. \tag{8}$$

$D^{e\varphi\varphi}$ was determined from the slope of the linearised plot of ln (MR) versus time. Activation energy (E_a) was subsequently determined using the Arrhenius equation [36]

$$D^{e\varphi\varphi} = D_0 \cdot e^{-\frac{E_a}{RT}}, \tag{9}$$

where D_0 is the pre-exponential factor (m^2/s); R is the universal gas constant (8.314 J/mol·K); T is the absolute drying air temperature (K). E_a was obtained from the slope of the Arrhenius plot of ln ($D^{e\varphi\varphi}$) versus 1/T. This approach is well-established in biomass drying research and has been applied to materials including poplar sawdust [27], rice husk [37], wheat straw [38], and castor oil seeds [32].

2 Results and discussion

2.1 Moisture transfer characteristics

The temporal variation in particle weight at the three drying temperatures is presented in Fig. 2. The initial saturated weight of the single Sal particle prior to each experiment was 10.235 g. Over the 360-minute drying period, the particle weight decreased to 4.970 g, 4.371 g, and 4.115 g at 75°C, 90°C, and 105°C, respectively. Across all temperatures, a steep weight reduction is observed during the initial drying period, which progressively diminishes as the experiment proceeds. This pattern is characteristic of internal diffusion-controlled drying in hygroscopic porous solids [20]. As temperature increases, the vapour pressure gradient between the particle interior and the surrounding air increases, accelerating moisture evaporation and reducing

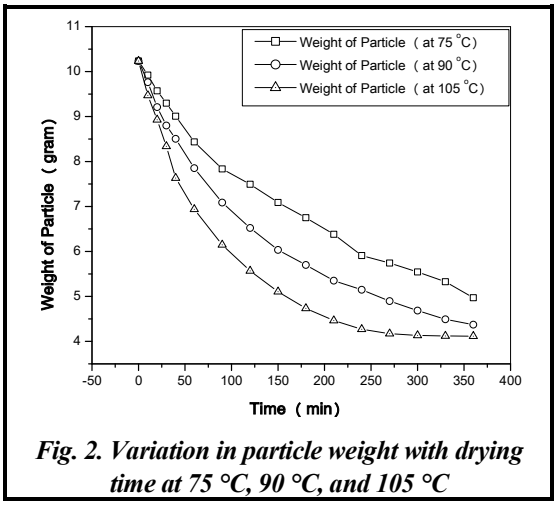


Fig. 2. Variation in particle weight with drying time at 75 °C, 90 °C, and 105 °C

the time required to reach a given moisture level [27]. It is worth noting that all three drying temperatures remain well below 200°C, the threshold at which volatile matter release from biomass becomes significant [39]; no thermal degradation of the samples therefore occurred during the experiments.

The variation in moisture content (dry basis) with drying time is shown in Fig. 3. Moisture migrates from the particle interior to its surface via thermally driven conduction and is subsequently removed from the surface by combined convection and radiation. On a wet basis, the final moisture content after 360 minutes of drying was 0.212, 0.066, and 0.004 at 75 °C, 90 °C, and 105 °C, respectively, confirming substantially complete drying at the highest temperature. These values are consistent with the target moisture range of 10–15 wt% (wet basis) required for combustion applications [15], confirming the practical utility of hot air oven drying at these temperatures for biomass fuel preparation.

The corresponding moisture ratio profiles are presented in Fig. 4. *MR* decreased continuously from unity to 0.142, 0.044, and 0.002 at 75 °C, 90 °C, and 105 °C, respectively, over the 360-minute drying period. No constant-rate drying period was observed at any temperature: the entire drying process occurred exclusively in the falling rate period, demonstrating that internal moisture diffusion rather than external mass transfer resistance governs the drying rate throughout [20, 28]. This finding is consistent with reported behaviour for other dense hardwood species and compact biomass particles [29, 30].

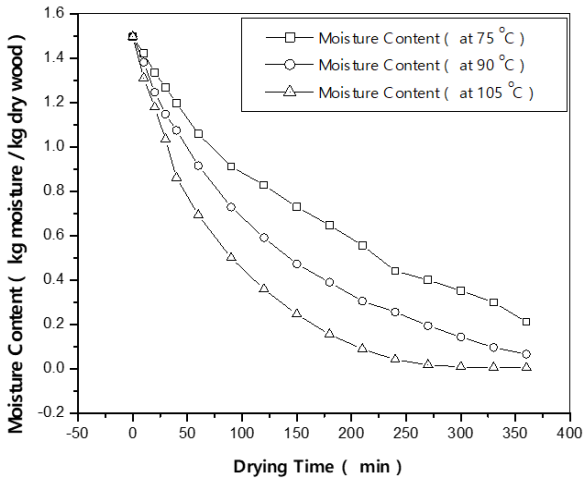


Fig. 3. Variation in moisture content with drying time at 75 °C, 90 °C, and 105 °C

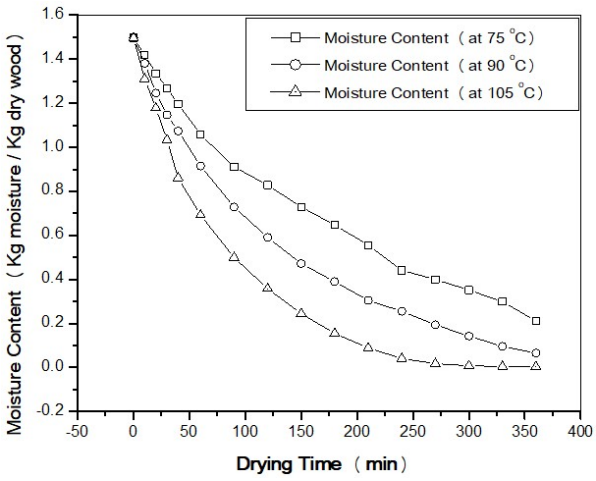


Fig. 4. Variation in moisture ratio with drying time at 75 °C, 90 °C, and 105 °C

2.2 Thin-layer drying model fitting and selection

The experimental *MR* data were fitted to the five thin-layer drying models listed in Table 1 using MATLAB curve fitting. The resulting model constants and statistical goodness-of-fit parameters at each temperature are compiled in Table 2. All five models achieved acceptable fits (R^2>0.95) across the three temperatures, confirming that the general form of the exponential drying equations is appropriate for Sal wood. However, marked differences in statistical performance exist between models.

The Page model consistently provided the best statistical fit at all three temperatures, with the highest R^2 values (0.9971 at 75 °C; 0.9988 at 90 °C; 0.9983 at 105 °C) and the lowest *SSE* (0.003618; 0.001854; 0.003047) and *RMSE* (0.01608; 0.01151; 0.01425) values. The Page model constant "*n*" ranged from 0.939 to 1.002 across the three temperatures, values close to unity, indicating that the drying kinetics are approximately exponential but with a slight non-linearity that the Lewis model (n=1) cannot capture. The Lewis model, while simpler, performed nearly as well at 90 °C and 105 °C (R^2=0.9982–0.9983), but was weaker at 75 °C (R^2=0.9955). The Wang & Singh model showed the poorest performance, with the lowest R^2 (0.9011 at 75 °C) and highest *RMSE* values, indicating that its polynomial form is unsuitable for describing the monotonically decaying *MR* profile of Sal wood. Henderson & Pabis and Modified Page performed similarly to the Lewis model.

The superiority of the Page model for woody biomass drying is consistent with the findings of Sridhar and Madhu [28] for *Casuarina* wood chips, Phanphanich and Mani [33] for pine forest residues, and

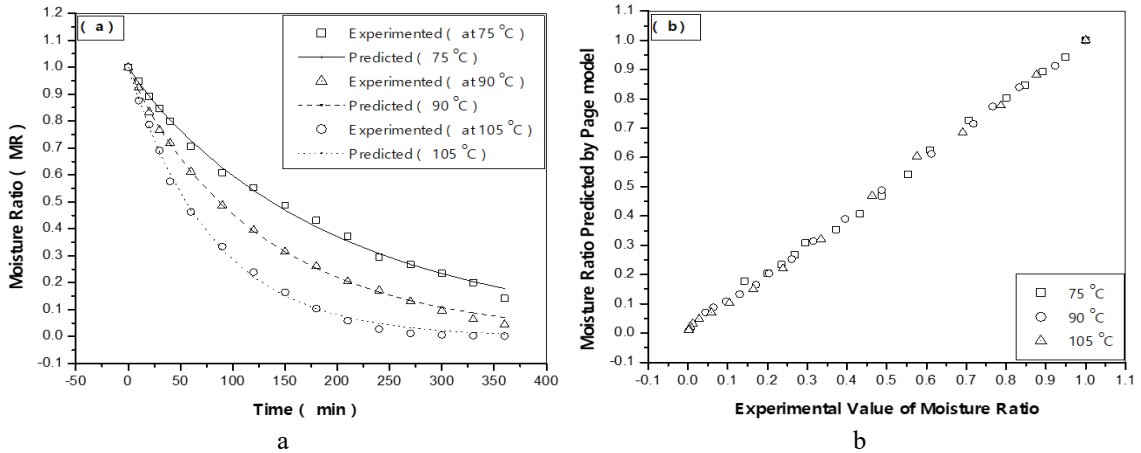
Perea-Flores et al. [32] for castor oil seeds, as well as the comprehensive review of Gandía-Ventura et al. [20], who identified the Page model as the most broadly applicable model for wood biomass drying under convective conditions. The additional empirical parameter "*n*" in the Page model affords greater flexibility to capture the curvature of the falling-rate drying curve, which may reflect the heterogeneous, hierarchical pore structure of Sal wood influencing moisture migration at different time scales.

Table 2. Statistical analysis of drying kinetic models for single Sal wood particles

Model	Temperature, °C	Model Constants	SSE	RMSE	R^2
Lewis	75	k=0.004877	0.005537	0.01921	0.9955
	90	k=0.007741	0.000291	0.01393	0.9982
	105	k=0.01263	0.003049	0.01426	0.9983
Page*	75	k=0.006734, n=0.9424	0.003618	0.01608	**0.9971**
	90	k=0.010490, n=0.9391	0.001854	0.01151	0.9988
	105	k=0.012510, n=1.0020	0.003047	0.01425	0.9983
Modified Page	75	k=0.725, n=0.006727	0.005537	0.01989	0.9955
	90	k=0.007861, n=0.9550	0.001632	0.01208	0.9986
	105	k=0.012630, n=1.0020	0.003047	0.01475	0.9983
Wang & Singh	75	k= −0.004299, k_1=5.68×10^{-6}	0.01230	0.02964	0.9011
	90	k= −0.006120, k_1=1.036×10^{-5}	0.03037	0.04658	0.9811
	105	k= −0.007925, k_1=1.502×10^{-5}	0.07403	0.07272	0.9596
Henderson & Pabis	75	k=0.00481, a=0.9821	0.004116	0.01715	0.9967
	90	k=0.00749, a=0.9688	0.002723	0.01395	0.9983
	105	k=0.01261, a=0.9986	0.003045	0.01475	0.9983

** Best-fit model selected on the basis of highest R² and lowest SSE and RMSE*

The fitted Page model curves are compared with the experimental *MR* data in Fig. 5, a, and the corresponding parity plot (predicted vs. experimental *MR*) is presented in Fig. 5, b. The close agreement between predicted and experimental values at all three temperatures confirms the adequacy of the Page model for describing the drying kinetics of Sal wood particles under the conditions studied. The drying rate constant *k* of the Page model increased with temperature (0.006734 at 75 °C; 0.01049 at 90 °C; 0.01251 at 105 °C), as expected from the Arrhenius temperature dependence of diffusion-controlled processes [20, 27].



a b

Fig. 5. Experimental and Page model-predicted moisture ratio versus drying time at 75 °C, 90 °C, and 105 °C (a); Parity plot of predicted versus experimental moisture ratio (b)

2.3 Effective moisture diffusivity

Since the drying of Sal wood occurred exclusively in the falling rate period, Fick's second law of diffusion for cylindrical geometry is the appropriate model for estimating $D^{эфф}$ [35]. The linearised plots of ln (*MR*) versus drying time at the three temperatures are shown in Fig. 6, from which the slopes ($-\pi^2 D^{эфф}/4h^2$) were extracted by linear regression. The calculated $D^{эфф}$ values were: 7.92×10^{-8} m^2/s at 75 °C, 12.67×10^{-8} m^2/s at 90 °C, and 26.0×10^{-8} m^2/s at 105 °C respectively.

These values lie within the reported range of 10^{-3} to 10^{-6} m^2/s for biological and lignocellulosic materials [35] and are physically reasonable for a dense tropical hardwood. $D^{эфф}$ increased by approximately 3.3-fold across the 30 °C temperature interval studied, reflecting the exponential (Arrhenius) sensitivity of molecular diffusion in the wood matrix to temperature. This non-linear relationship between $D^{эфф}$ and temperature, visible in Fig. 7, a, is characteristic of thermally activated transport processes in porous biopolymer matrices [36].

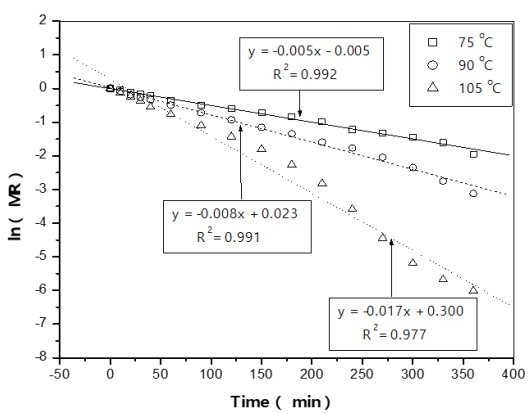
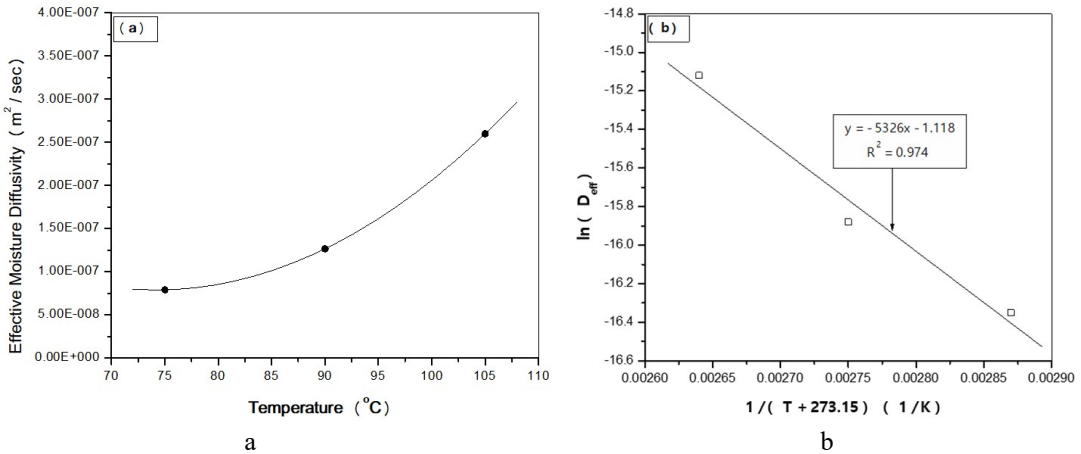


Fig. 6. Linearised plot of ln (MR) versus drying time at 75 °C, 90 °C, and 105 °C for estimation of effective moisture diffusivity

2.4 Activation energy and arrhenius analysis

The Arrhenius plot of ln($D^{эфф}$) versus the reciprocal of the absolute drying temperature ($1/T$ in K^{-1}) is presented in Fig. 7, b. A strong linear relationship (R^2=0.974) was obtained, from which the activation energy of moisture diffusion in Sal wood was calculated as 4.42×10^4 J/mol across the experimental temperature range of 75–105°C. This value represents the minimum energy barrier that must be overcome for moisture molecules to migrate through the wood matrix and is a key parameter for dryer design and scale-up.

A comparison of the activation energy of Sal wood with those reported in the literature for other biomass materials is presented in Table 3. The activation energy of Sal wood (4.42×10^4 J/mol) is higher than those reported for rice husk [37], poplar sawdust [27], and wheat straw [38], which range from 1.18 to 1.41×10^4 J/mol. This higher value is consistent with the dense, resinous microstructure of Sal wood, which is known to have a low porosity and a high density relative to other biomass feedstocks [40], imposing a greater resistance to moisture transport. The activation energy value is also in good agreement with the range of 20–60 kJ/mol commonly reported for convective drying of solid biomass materials [20]. Knowledge of E_a is particularly valuable for dryer modelling, since it enables the drying rate constant k to be predicted at temperatures other than those experimentally studied, facilitating the simulation and optimisation of industrial drying systems.



a b

Fig. 7. Effective moisture diffusivity as a function of drying temperature (a); Arrhenius plot of ln($D^{эфф}$) versus reciprocal absolute temperature (b)

Table 3. Comparison of activation energy of Sal wood with other biomass materials

Biomass material	Temperature range, °C	E_a, J/mol	Reference
Sal (Shorea robusta) wood – present study	75–105	4.42×10^4	This paper
Poplar sawdust	50–90	1.23×10^4	Chen et al. [27]
Rice husk	50–90	1.18×10^4	Chen et al. [37]
Wheat straw	50–90	1.41×10^4	Cai & Chen [38]
Casuarina wood chips	50–100	~2.10×10^4	Sridhar & Madhu [28]

Conclusions

The drying kinetics, effective moisture diffusivity, and activation energy of single cylindrical *Shorea robusta* (Sal) wood particles have been experimentally determined for the first time under isothermal hot air oven conditions at 75 °C, 90 °C, and 105 °C. The following principal conclusions are drawn from this study:

1. The drying of Sal wood occurred exclusively in the falling rate period at all three temperatures, confirming that internal moisture diffusion, not surface evaporation, is the rate-controlling mechanism. No constant-rate drying period was observed.

2. All five thin-layer drying models tested achieved acceptable fits (R^2>0.95), but the Page model provided the best statistical performance overall, with R^2=0.9971, 0.9988, and 0.9983; *SSE*=0.003618, 0.001854, and 0.003047; and *RMSE*=0.01608, 0.01151, and 0.01425 at 75 °C, 90 °C, and 105 °C, respectively. This outcome is consistent with the broad literature on wood biomass drying.

3. Effective moisture diffusivity increased with drying temperature: 7.92×10^{-8}, 12.67×10^{-8}, and 26.0×10^{-8} m^2/s at 75 °C, 90 °C, and 105 °C, respectively. The approximately 3.3-fold increase over the 30 °C temperature range reflects the Arrhenius sensitivity of moisture diffusion in the dense Sal wood matrix.

4. Activation energy was found to be 4.42×10^4 J/mol (Arrhenius R^2=0.974), which is higher than values reported for less dense biomass materials such as rice husk, poplar sawdust, and wheat straw, consistent with the characteristically low porosity and high density of Sal timber.

5. At 105 °C, the final moisture content achieved after 360 minutes was approximately 0.4 wt% (wet basis), well within the target range of 10–15 wt% for direct combustion applications, demonstrating the practical efficacy of hot air oven drying at this temperature for Sal wood fuel preparation.

The Page model constants and Arrhenius parameters obtained in this study can be directly applied in the simulation and optimisation of industrial hot air dryers for Sal wood biomass processing. Future research should investigate the effect of particle size and initial moisture content on drying kinetics, explore alternative dryer technologies (solar, fluidised bed, superheated steam), and extend the temperature range to fully delineate the transition from bound-water diffusion to combined diffusion-evaporation mechanisms.

Acknowledgement

The authors express their sincere gratitude to the Bhagwant University, Ajmer, Rajasthan; and Polytechnic Sahjanwa, Gorakhpur for their support in carrying out this research paper.

Nomenclature and

W^b – wet particle mass, g;
W^d – dry particle mass, g;
M_0 – initial moisture content (dry basis);
M_e – equilibrium moisture content;
M_t – moisture content at time t;
MC – moisture content, %;
MR – moisture ratio;
SSE – sum of squares of error;
RMSE – root mean square error;
R^2 – coefficient of determination;
k, k_1 – drying rate constants;
t – drying time, s or min;
MR_i^{cal} – predicted moisture ratio;
MR_i^{exp} – experimental moisture ratio;
N – total number of observations;
n – number of model parameters;
D^{eff} – effective moisture diffusivity, m^2/s;
D_0 – pre-exponential factor, m^2/s;
T – absolute temperature, K;
E_a – activation energy, J/mol;
R – universal gas constant, 8.314 J/mol·K;
h – half-thickness of cylinder, m;
a, n – model constants

References

1. (2023). REN21. *Renewables 2023 Global Status Report*. REN21 Secretariat, Paris, France. https://www.ren21.net/gsr-2023/.
2. (2023). International Energy Agency (IEA). *World Energy Outlook 2023*. IEA Publications, Paris, France. https://doi.org/10.1787/827374a6-en.
3. Basu, P. (2018). Biomass gasification, pyrolysis and torrefaction: Practical design and theory (3rd ed.) *Practical Design and Theory*, pp. 211–262. https://doi.org/10.1016/B978-0-12-812992-0.00007-8.
4. Bardalai, M. & Mahanta, D. K. (2016). Production of pyrolysis oil from Areca tree using a fixed bed reactor. *Journal of Engineering Research*, vol. 4, iss. 2, pp. 172–187. https://doi.org/10.1016/S2307-1877(25)00887-9.
5. Verma, M., Loha, C., Sinha, A. N., & Chatterjee, P. K. (2017). Drying of biomass for utilising in co-firing with coal and its impact on environment – A review. *Renewable and Sustainable Energy Reviews*, vol. 71, pp. 732–741. https://doi.org/10.1016/j.rser.2016.12.101.
6. Riaza, J., Álvarez, L., Gil, M. V., Pevida, C., Pis, J. J., & Rubiera, F. (2013). Ignition and NO emissions of coal and biomass blends under different oxy-fuel atmospheres. *Energy Procedia*, vol. 37, pp. 1405–1412. https://doi.org/10.1016/j.egypro.2013.06.016.
7. Luk, H. T., Lam, T. Y. G., Oyedun, A. O., Gebreegziabher, T., & Hui, C. W. (2013). Drying of biomass for power generation: A case study on power generation from empty fruit bunch. *Energy*, vol. 63, pp. 205–215. https://doi.org/10.1016/j.energy.2013.10.056.
8. Liu, Y., Peng, J., Kansha, Y., Ishizuka, M., Tsutsumi, A., Jia, D., Bi, X. T., Lim, C. J., & Sokhansanj, S. (2014). Novel fluidized bed dryer for biomass drying. *Fuel Processing Technology*, vol. 122, pp. 170–175. https://doi.org/10.1016/j.fuproc.2014.01.036.
9. Gautam, K. H. & Devoe, N. N. (2006). Ecological and anthropogenic niches of sal (*Shorea robusta* Gaertn. f.) forest and prospects for multiple-product forest management – A review. *Forestry*, vol. 79, iss. 1, pp. 81–101. https://doi.org/10.1093/forestry/cpi063.
10. Singh, S. & Gupta, A. (2014). Comparative fermentation studies on amylase production by *Aspergillus flavus* TF-8 using Sal (*Shorea robusta*) deoiled cake. *Industrial Crops and Products*, vol. 57, pp. 158–165. https://doi.org/10.1016/j.indcrop.2014.03.035.
11. Deka, J., Tripathi, O. P., & Khan, M. L. (2012). High dominance of *Shorea robusta* Gaertn. in alluvial plain Kamrup sal forest of Assam, N.E. India. *International Journal of Ecosystem*, vol. 2, iss. 4, pp. 67–73. https://doi.org/10.5923/j.ije.20120204.04.
12. Dimri, R., Majhi, S., Das, K., & Kumar, S. (2026). Distribution, utilization, and ecological services of Sal (*Shorea robusta* C. F. Gaertn.). *Indian Forester*, vol. 152, iss. 5, pp. 426–433. https://doi.org/10.36808/if/2026/v152i5/171045.
13. Pradhan, R. R., Garnaik, P. P., Regmi, B., Dash, B., & Dutta, A. (2017). Pyrolysis kinetics of Sal (*Shorea robusta*) seeds. *Biomass Conversion and Biorefinery*, vol. 7, iss. 2, pp. 237–246. https://doi.org/10.1007/s13399-017-0240-3.
14. Behera, S. K. & Misra, M. K. (2006). Aboveground tree biomass in a recovering tropical Sal (*Shorea robusta* Gaertn. f.) forest of Eastern Ghats, India. *Biomass and Bioenergy*, vol. 30, iss. 6, pp. 509–521. https://doi.org/10.1016/j.biombioe.2006.01.003.
15. Eliaers, P. & De Wilde, J. (2013). Drying of biomass particles: experimental study and comparison of a conventional fluidized bed and a rotating fluidized bed in a static geometry. *Drying Technology*, vol. 31, iss. 2, pp. 236–245. https://doi.org/10.1080/07373937.2012.726304.
16. Haque, N. & Somerville, M. (2013). Techno-economic and environmental evaluation of biomass dryer. *Procedia Engineering*, vol. 56, pp. 650–655. https://doi.org/10.1016/j.proeng.2013.03.173.
17. Lee, H. W. (2006). Study on the fluidized bed drying characteristics of sawdust as a raw material for wood-pellet fuel. *Journal of the Korean Wood Science and Technology*, vol. 34, iss. 2, pp. 30–36.
18. Demirbas, A. (2004). The importance of biomass. *Energy Sources*, vol. 26, iss. 4, pp. 361–366. https://doi.org/10.1080/00908310490774 06.
19. Castagna, A. & Rein, G. (2025). Surrogate chemical kinetics for drying of biomass and influence of moisture content on the burning behaviour of wood. *Proceedings of the Combustion Institute*, vol. 41, article 105985. https://doi.org/10.1016/j.proci.2025.105985.
20. Gandía-Ventura, I., Velázquez-Martí, B., López-Cortés, I., & Guerrero-Luzuriaga, S. (2024). Kinetic models of wood biomass drying in hot airflow systems. *Applied Sciences*, vol. 14, iss. 15, article 6716. https://doi.org/10.3390/app14156716.
21. Arabi, M. & Dahmardeh Ghalehno, M. (2026). Thin-layer drying models and artificial neural network for wood fiber drying. *BioResources*, vol. 21, iss. 1, pp. 654–672. https://doi.org/10.15376/biores.21.1.654-672.
22. Núñez-Retana, V. D., Carrillo-Parra, A., Escobar Machado, J. A., Moposita-Vasquez, D.-D., & Velázquez-Martí, B. (2025). Predictive models for the convective drying kinetics of *Pinus* spp. energy wood chips. *Applied Sciences*, vol. 15, iss. 18, article 10081. https://doi.org/10.3390/app151810081.

23. Mihindukulasuriya, S. D. F. &. Jayasuriya, H. P. W. (2013). Mathematical modelling of drying characteristics of chilli in hot air oven and fluidized bed dryers. *Agricultural Engineering International: CIGR Journal*, vol. 15, iss. 1, pp. 154–166.
24. Safeena, A. & Patil, S. (2013). Effect of hot air oven and microwave oven drying on production of quality dry flowers of Dutch roses. *Journal of Agricultural Science*, vol. 5, no. 4, pp. 179–189. https://doi.org/10.5539/jas.v5n4p179.
25. Upadhyaya, A., Gupta, B., Garg, S., Singh, M. B., & Pandey, M. (2012). Mathematical modelling of hot air drying of spinach leaves in universal hot air oven. *International Journal of Advanced Research in Computer Engineering & Technology*, vol. 1, iss. 4, pp. 153–157.
26. Faisal, S., Tabassum, R., & Kumar, V. (2013). Performance evaluation and process optimisation of potato drying using hot air oven. *Journal of Food Processing Technology*, vol. 4, iss. 10, article 273. https://doi.org/10.4172/2157-7110.1000273.
27. Chen, D., Zheng, Y., & Zhu, X. (2012). Determination of effective moisture diffusivity and drying kinetics for poplar sawdust by thermogravimetric analysis under isothermal condition. *Bioresource Technology*, vol. 107, pp. 451–455. https://doi.org/10.1016/j.biortech.2011.12.032.
28. Sridhar, D. & Madhu, G. M. (2015). Drying kinetics and mathematical modelling of *Casuarina equisetifolia* wood chips at various temperatures. *Periodica Polytechnica Chemical Engineering*, vol. 59, no. 4, pp. 288–295. https://doi.org/10.3311/PPch.7855.
29. Kuznetsov, G. V., Syrodoy, S. V., Nigay, N. A., Maksimov, V. I., & Gutareva, N. Y. (2021). Features of heat and mass transfer during drying of large-thickness wood biomass layers. *Renewable Energy*, vol. 169, pp. 498–511. https://doi.org/10.1016/j.renene.2020.12.137.
30. Núñez-Retana, V. D., Carrillo-Parra, A., Moposita-Vasquez, D.-D., & Velázquez-Martí, B. (2026). Analysis of convective drying in particles of pine wood chips for bioenergy. *Biomass Conversion and Biorefinery*, vol. 16, iss. 3, article 96. https://doi.org/10.1007/s13399-025-06957-z.
31. Loha, C., Das, R., Choudhury, B., Chatterjee, P. K. (2012). Evaluation of air drying characteristics of sliced ginger (*Zingiber officinale*) in a forced convective cabinet dryer and thermal conductivity measurement. *Journal of Food Processing Technology*, vol. 6, iss. 3, article 160. https://doi.org/10.4172/2157-7110.1000160.
32. Perea-Flores, M. J., Garibay-Febles, V., Chanona-Pérez, J. J., Calderón-Domínguez, G., Méndez-Méndez, J. V., Palacios-González, E., & Gutiérrez-López, G. F. (2012). Mathematical modelling of castor oil seeds (*Ricinus communis*) drying kinetics in fluidized bed at high temperatures. *Industrial Crops and Products*, vol. 38, pp. 64–71. https://doi.org/10.1016/j.indcrop.2012.01.008.
33. Phanphanich, M. & Mani, S. (2010). Drying kinetics of pine forest residues. *BioResources*, vol. 5, iss. 1, pp. 108–121. https://doi.org/10.15376/biores.5.1.108-120.
34. Jan, K., Riar, C. S., & Saxena, D. C. (2014). Mathematical modelling of thin layer drying kinetics of biodegradable pellets. *Journal of Food Processing Technology*, vol. 5, iss. 9, article 370. https://doi.org/10.4172/2157-7110.1000370.
35. Borah, A., Hazarika, K., & Khayer, S. M. (2015). Drying kinetics of whole and sliced turmeric rhizomes (*Curcuma longa* L.) in a solar conduction dryer. *Information Processing in Agriculture*, vol. 2, iss. 2, pp. 85–92. https://doi.org/10.1016/j.inpa.2015.06.002.
36. Taheri-Garavand, A., Rafiee, S., & Keyhani, A. (2011). Effective moisture diffusivity and activation energy of tomato in thin layer dryer during hot air drying. *International Transaction Journal of Engineering, Management & Applied Sciences and Technologies*, vol. 2, no. 2, pp. 239–248.
37. Chen, D., Liu, X., & Zhu, X. (2013). A one-step non-isothermal method for the determination of effective moisture diffusivity in powdered biomass. *Biomass and Bioenergy*, vol. 50, pp. 81–86. https://doi.org/10.1016/j.biombioe.2013.01.023.
38. Cai, J. & Chen, S. (2008). Determination of drying kinetics for biomass by thermogravimetric analysis under non-isothermal condition. *Drying Technology*, vol. 26, iss. 12, pp. 1464–1468. https://doi.org/10.1080/07373930802412116.
39. Gómez-de la Cruz, F. J., Cruz-Peragón, F., Casanova-Peláez, P. J., & Palomar-Carnicero, J. M. (2015). A vital stage in the large-scale production of biofuels from spent coffee grounds: The drying kinetics. *Fuel Processing Technology*, vol. 130, pp. 188–196. https://doi.org/10.1016/j.fuproc.2014.10.012.
40. Valente, C., Spinelli, R., Hillring, B. G., & Solberg, B. (2014). Mountain forest wood fuel supply chains: comparative studies between Norway and Italy. *Biomass and Bioenergy*, vol. 71, pp. 370–380. https://doi.org/10.1016/j.biombioe.2014.09.018.

Received 18 July 2026 *Accepted 26 August 2026* *Published 30 September 2026*

Кінетика сушіння циліндричного зразка деревини сал (Shorea robusta): коефіцієнт дифузії вологи, енергія активації та значення для біоенергетики

[1] M. Verma, [2] R. K. Ranjan

[1] Університет Бхагванта, Ajmer-305004, Rajasthan, Індія

[2] Урядова політехніка Сахджанва, Gorakhpur – 273209, Uttar Pradesh, Індія

У цій статті досліджується кінетика ізотермічного сушіння та ефективний коефіцієнт дифузії вологи у циліндричних зразках деревини сал (Shorea robusta), висушених у сушильній шафі гарячим повітрям за температур 75 °C, 90 °C та 105 °C. Деревина сал – це одна з найбільш екологічно та комерційно значущих листяних порід Індійського субконтиненту, має значні перспективи як біопаливна сировина, проте її характеристики сушіння досі систематично не досліджувалися. П'ять відомих моделей тонкошарового сушіння – Lewis, Page, Modified Page, Wang & Singh та Henderson & Pabis – було апроксимовано до експериментальних даних відносного вологовмісту (MR) за допомогою засобів апроксимації кривих у MATLAB. Модель Page забезпечила найкращу статистичну відповідність, при цьому коефіцієнти детермінації (R^2) становили 0,9971, 0,9988 та 0,9983; значення суми квадратів похибок (SSE) – 0,003618, 0,001854 та 0,003047; значення середньоквадратичної похибки (RMSE) – 0,01608, 0,01151 та 0,01425 при 75°C, 90°C та 105°C відповідно. Ефективний коефіцієнт дифузії вологи, розрахований за допомогою аналітичного розв'язку другого закону Фіка для циліндричної геометрії, збільшився з $7{,}92\times10^{-8}$ до $26{,}0\times10^{-8}$ м²/с у досліджуваному діапазоні температур. Енергія активації, оцінена за допомогою рівняння Арреніуса, становила $4{,}42\times10^{4}$Дж/моль, що узгоджується зі значеннями, отриманими для аналогічних лігноцелюлозних біомас. Отримані результати надають фундаментальні кінетичні дані для раціонального проєктування сушарок та оптимізації систем попередньої обробки біомаси.

***Ключові слова**: енергія активації, кінетика сушіння ефективний коефіцієнт дифузії вологи, шафа з гарячим повітрям, тонкошарове сушіння.*

Література

1. REN21. *Renewables 2023 Global Status Report*. REN21 Secretariat, Paris, France, 2023. https://www.ren21.net/gsr-2023/.
2. International Energy Agency (IEA). *World Energy Outlook 2023*. IEA Publications, Paris, France, 2023. https://doi.org/10.1787/827374a6-en.
3. Basu P. Biomass gasification, pyrolysis and torrefaction: Practical design and theory (3rd ed.) *Practical Design and Theory*. 2018. P. 211–262. https://doi.org/10.1016/B978-0-12-812992-0.00007-8.
4. Bardalai M., Mahanta D. K. Production of pyrolysis oil from Areca tree using a fixed bed reactor. *Journal of Engineering Research*. 2016. Vol. 4. Iss. 2. P. 172–187. https://doi.org/10.1016/S2307-1877(25)00887-9.
5. Verma M., Loha C., Sinha A. N., Chatterjee P. K. Drying of biomass for utilising in co-firing with coal and its impact on environment – A review. *Renewable and Sustainable Energy Reviews*. 2017. Vol. 71. P. 732–741. https://doi.org/10.1016/j.rser.2016.12.101.
6. Riaza J., Álvarez L., Gil M. V., Pevida C., Pis J. J., Rubiera F. Ignition and NO emissions of coal and biomass blends under different oxy-fuel atmospheres. *Energy Procedia*. 2013. Vol. 37. P. 1405–1412. https://doi.org/10.1016/j.egypro.2013.06.016.
7. Luk H. T., Lam T. Y. G., Oyedun A. O., Gebreegziabher T., Hui C. W. Drying of biomass for power generation: A case study on power generation from empty fruit bunch. *Energy*. 2013. Vol. 63. P. 205–215. https://doi.org/10.1016/j.energy.2013.10.056.
8. Liu Y., Peng J., Kansha Y., Ishizuka M., Tsutsumi A., Jia D., Bi X. T., Lim C. J., Sokhansanj S. Novel fluidized bed dryer for biomass drying. *Fuel Processing Technology*. 2014. Vol. 122. P. 170–175. https://doi.org/10.1016/j.fuproc.2014.01.036
9. Gautam K. H., Devoe N. N. Ecological and anthropogenic niches of sal (*Shorea robusta* Gaertn. f.) forest and prospects for multiple-product forest management – A review. *Forestry*. 2006. Vol. 79. Iss. 1. P. 81–101. https://doi.org/10.1093/forestry/cpi063.
10. Singh S., Gupta A. Comparative fermentation studies on amylase production by *Aspergillus flavus* TF-8 using Sal (*Shorea robusta*) deoiled cake. *Industrial Crops and Products*. 2014. Vol. 57. P. 158–165. https://doi.org/10.1016/j.indcrop.2014.03.035.

11. Deka J., Tripathi O. P., Khan M. L. High dominance of *Shorea robusta* Gaertn. in alluvial plain Kamrup sal forest of Assam, N.E. India. *International Journal of Ecosystem*. 2012. Vol. 2. Iss. 4. P. 67–73. https://doi.org/10.5923/j.ije.20120204.04.
12. Dimri R., Majhi S., Das K., Kumar S. Distribution, utilization, and ecological services of Sal (*Shorea robusta* C. F. Gaertn.). *Indian Forester*. 2026. Vol. 152. Iss. 5. P. 426–433. https://doi.org/10.36808/if/2026/v152i5/171045.
13. Pradhan R. R., Garnaik P. P., Regmi B., Dash B., Dutta A. Pyrolysis kinetics of Sal (*Shorea robusta*) seeds. *Biomass Conversion and Biorefinery*. 2017. Vol. 7. Iss. 2. P. 237–246. https://doi.org/10.1007/s13399-017-0240-3.
14. Behera S. K., Misra M. K. Aboveground tree biomass in a recovering tropical Sal (*Shorea robusta* Gaertn. f.) forest of Eastern Ghats, India. *Biomass and Bioenergy*. 2006. Vol. 30. Iss. 6. P. 509–521. https://doi.org/10.1016/j.biombioe.2006.01.003.
15. Eliaers P., De Wilde J. Drying of biomass particles: experimental study and comparison of a conventional fluidized bed and a rotating fluidized bed in a static geometry. *Drying Technology*. 2013. Vol. 31. Iss. 2. P. 236–245. https://doi.org/10.1080/07373937.2012.726304.
16. Haque N., Somerville M. Techno-economic and environmental evaluation of biomass dryer. *Procedia Engineering*. 2013. Vol. 56. P. 650–655. https://doi.org/10.1016/j.proeng.2013.03.173.
17. Lee H. W. Study on the fluidized bed drying characteristics of sawdust as a raw material for wood-pellet fuel. *Journal of the Korean Wood Science and Technology*. 2006. Vol. 34. Iss. 2. P. 30–36.
18. Demirbas A. The importance of biomass. *Energy Sources*. 2004. Vol. 26. Iss. 4. P. 361–366. https://doi.org/10.1080/00908310490774 06.
19. Castagna A., Rein G. Surrogate chemical kinetics for drying of biomass and influence of moisture content on the burning behaviour of wood. *Proceedings of the Combustion Institute*. 2025. Vol. 41. Article 105985. https://doi.org/10.1016/j.proci.2025.105985.
20. Gandía-Ventura I., Velázquez-Martí B., López-Cortés I., Guerrero-Luzuriaga S. Kinetic models of wood biomass drying in hot airflow systems. *Applied Sciences*. 2024. Vol. 14. Iss. 15. Article 6716. https://doi.org/10.3390/app14156716.
21. Arabi M., Dahmardeh Ghalehno M. Thin-layer drying models and artificial neural network for wood fiber drying. *BioResources*. 2026. Vol. 21. Iss. 1. P. 654–672. https://doi.org/10.15376/biores.21.1.654-672.
22. Núñez-Retana V. D., Carrillo-Parra A., Escobar Machado J. A., Moposita-Vasquez D.-D., Velázquez-Martí B. Predictive models for the convective drying kinetics of *Pinus* spp. energy wood chips. *Applied Sciences*. 2025. Vol. 15. Iss. 18. Article 10081. https://doi.org/10.3390/app151810081.
23. Mihindukulasuriya S. D. F., Jayasuriya H. P. W. Mathematical modelling of drying characteristics of chilli in hot air oven and fluidized bed dryers. *Agricultural Engineering International: CIGR Journal*. 2013. Vol. 15. Iss. 1. P. 154–166.
24. Safeena A., Patil S. Effect of hot air oven and microwave oven drying on production of quality dry flowers of Dutch roses. *Journal of Agricultural Science*. 2013. Vol. 5. No. 4. P. 179–189. https://doi.org/10.5539/jas.v5n4p179.
25. Upadhyaya A., Gupta B., Garg S., Singh M. B., Pandey M. Mathematical modelling of hot air drying of spinach leaves in universal hot air oven. *International Journal of Advanced Research in Computer Engineering & Technology*. 2012. Vol. 1. Iss. 4. P. 153–157.
26. Faisal S., Tabassum R., Kumar V. Performance evaluation and process optimisation of potato drying using hot air oven. *Journal of Food Processing Technology*. 2013. Vol. 4. Iss. 10. Article 273. https://doi.org/10.4172/2157-7110.1000273.
27. Chen D., Zheng Y., Zhu X. Determination of effective moisture diffusivity and drying kinetics for poplar sawdust by thermogravimetric analysis under isothermal condition. *Bioresource Technology*. 2012. Vol. 107. P. 451–455. https://doi.org/10.1016/j.biortech.2011.12.032.
28. Sridhar D., Madhu G. M. Drying kinetics and mathematical modelling of *Casuarina equisetifolia* wood chips at various temperatures. *Periodica Polytechnica Chemical Engineering*. 2015. Vol. 59. No. 4. P. 288–295. https://doi.org/10.3311/PPch.7855.
29. Kuznetsov G. V., Syrodoy S. V., Nigay N. A., Maksimov V. I., Gutareva N. Y. Features of heat and mass transfer during drying of large-thickness wood biomass layers. *Renewable Energy*. 2021. Vol. 169. P. 498–511. https://doi.org/10.1016/j.renene.2020.12.137.
30. Núñez-Retana V. D., Carrillo-Parra A., Moposita-Vasquez D.-D., Velázquez-Martí B. Analysis of convective drying in particles of pine wood chips for bioenergy. *Biomass Conversion and Biorefinery*. 2026. Vol. 16. Iss. 3. Article 96. https://doi.org/10.1007/s13399-025-06957-z.

31. Loha C., Das R., Choudhury B., Chatterjee P. K. Evaluation of air drying characteristics of sliced ginger (*Zingiber officinale*) in a forced convective cabinet dryer and thermal conductivity measurement. *Journal of Food Processing Technology*. 2012. Vol. 6. Iss. 3. Article 160. https://doi.org/10.4172/2157-7110.1000160.
32. Perea-Flores M. J., Garibay-Febles V., Chanona-Pérez J. J., Calderón-Domínguez G., Méndez-Méndez J. V., Palacios-González E., Gutiérrez-López G. F. Mathematical modelling of castor oil seeds (*Ricinus communis*) drying kinetics in fluidized bed at high temperatures. *Industrial Crops and Products*. 2012. Vol. 38. P. 64–71. https://doi.org/10.1016/j.indcrop.2012.01.008.
33. Phanphanich M., Mani S. Drying kinetics of pine forest residues. *BioResources*. 2010. Vol. 5. Iss. 1. P. 108–121. https://doi.org/10.15376/biores.5.1.108-120.
34. Jan K., Riar C. S., Saxena D. C. Mathematical modelling of thin layer drying kinetics of biodegradable pellets. *Journal of Food Processing Technology*. 2014. Vol. 5. Iss. 9. Article 370. https://doi.org/10.4172/2157-7110.1000370.
35. Borah A., Hazarika K., Khayer S. M. Drying kinetics of whole and sliced turmeric rhizomes (*Curcuma longa* L.) in a solar conduction dryer. *Information Processing in Agriculture*. 2015. Vol. 2. Iss. 2. P. 85–92. https://doi.org/10.1016/j.inpa.2015.06.002.
36. Taheri-Garavand A., Rafiee S., Keyhani A. Effective moisture diffusivity and activation energy of tomato in thin layer dryer during hot air drying. *International Transaction Journal of Engineering, Management & Applied Sciences and Technologies*. 2011. Vol. 2. No. 2. P. 239–248.
37. Chen D., Liu X., Zhu X. A one-step non-isothermal method for the determination of effective moisture diffusivity in powdered biomass. *Biomass and Bioenergy*. 2013. Vol. 50. P. 81–86. https://doi.org/10.1016/j.biombioe.2013.01.023.
38. Cai J., Chen S. Determination of drying kinetics for biomass by thermogravimetric analysis under non-isothermal condition. *Drying Technology*. 2008. Vol. 26. Iss. 12. P. 1464–1468. https://doi.org/10.1080/07373930802412116.
39. Gómez-de la Cruz F. J., Cruz-Peragón F., Casanova-Peláez P. J., Palomar-Carnicero J. M. A vital stage in the large-scale production of biofuels from spent coffee grounds: The drying kinetics. *Fuel Processing Technology*. 2015. Vol. 130. P. 188–196. https://doi.org/10.1016/j.fuproc.2014.10.012.
40. Valente C., Spinelli R., Hillring B. G., Solberg B. Mountain forest wood fuel supply chains: comparative studies between Norway and Italy. *Biomass and Bioenergy*. 2014. Vol. 71. P. 370–380. https://doi.org/10.1016/j.biombioe.2014.09.018.